STUDY AND IMPLEMENTATION OF A SIMPLIFIED AND EFFICIENT DIGITAL VECTOR CONTROLLER FOR INDUCTION MOTORS

D. Casadei - G. Grandi - G. Serra

UNIVERSITÀ DEGLI STUDI DI BOLOGNA - ITALY

ABSTRACT

This paper deals with the analysis and the implementation of a rotor flux oriented torque control for induction motors which utilises stator flux components as controlled variables. Combining the advantages of rotor flux orientation and stator flux space vector control leads to a high performance drive using a simple control scheme without the requirement for speed or position feedback. The strategy adopted needs neither the rotor resistance of the machine nor the co-ordinate transformation based on the rotor flux position. A simulation program has been developed in order to examine the behaviour of the overall drive system. The numerical results obtained in steady state and transient conditions confirm the expected drive performance. Some experimental results are also given.

INTRODUCTION

In recent years, control techniques for high-performance induction motor drives have been developed largely as alternative solutions to high-performance four-quadrant DC servo drives. Many schemes have been proposed but the field-oriented control has been accepted as one of the most effective methods. The input commands are torque and flux, while the output commands are three-phase reference currents. The torque command is usually generated from speed-loop controller, whereas the flux command is selected according to operation requirements. In many variable speed drives, such as traction drives, torque control is required without closed-loop control of speed. In this case, the torque command co nes directly from the user input. The flux and torque are estimated using various combinations of stator voltage, stator current, and shaft position or speed. In some applications the speed or position feedback is extremely difficult to obtain and the presence of a rotational transducer degrades the robustness of the drive system. Then, a torque control scheme which does not requires motor speed informations is very advantageous [1].

The rotor flux based field oriented control allows a complete decoupling of flux and torque control variables. In application of this type of field oriented control, the control variables are usually the stator current components. A torque command, at constant rotor flux, is followed instantaneously without transient rotor and stator currents.

The method proposed in [2] ,[3] is based on direct control of torque and stator flux. These quantities can be controlled independently by selecting a proper configuration of the inverter switches. The selection is made according to the instantaneous errors in torque and flux. This method results in a high performance AC servo system with quick torque response.

The scheme proposed in this paper is also based on direct control of the torque and stator flux, but the rotor flux and torque are assumed as references. Assuming the rotor flux as reference, the highest pull-out torque is obtained [4]. It is so possible to combine the advantages of rotor flux orientation and stator flux control without the need of determining the instantaneous position of the rotor flux. The strategy adopted needs neither the rotor resistance of the machine nor the coordinate transformation based on the rotor flux position, leading to a high performance drive using a simple control scheme.

The use of stator flux components as controlled variables allows to reduce the saturation effects in detuned operation. Furthermore a change in rotor flux command is followed with a time constant which is much lower than that involved in stator current control. It will be shown that this approach has the advantage of requiring motor parameters which are moderately affected by saturation.

A numerical simulation of the overall system has been carried out, taking into account the influence of technical problems linked with the processing of informations. Simulation results showing the transient response of the torque control are given.

For the realisation of the proposed control system, a DSP based processing system has been chosen. Some experimental results are also presented, which confirm the validity of the proposed control scheme.

MATHEMATICAL MODEL AND BASIC EQUATIONS

In order to obtain an accurate dynamic representation of the motor, it is necessary to base the calculation on the coupled circuit equations of induction machines. The equations are written in terms of d-q spatial vector, referred to a rotor reference frame

$$\vec{v}_s^r = R_s \vec{i}_s^r + p \vec{\Phi}_s^r + j \omega_m \vec{\Phi}_s^r \tag{1}$$

$$0 = R_r \vec{i}_r^r + p \vec{\Phi}_r^r \tag{2}$$

where

$$\vec{\Phi}_s^r = L_s \vec{i}_s^r + M \vec{i}_r^r \tag{3}$$

$$\vec{\Phi}_r^r = L_r \vec{i}_r^r + M \vec{i}_s^r \tag{4}$$

and

p differential operator (d/dt)
s,r superscripts denoting variables in stator and rotor reference frame respectively
s,r subscripts for stator and rotor quantities
L,M self and mutual inductance
R winding resistance
ω_m rotor electrical angular speed

The electromagnetic torque can be expressed as

$$T = P\,\bar{i}_s \cdot j\,\bar{\Phi}_s = -P\,\bar{i}_r \cdot j\,\bar{\Phi}_r \tag{5}$$

where P is the pole pair number.

In rotor-flux based field-oriented applications, the control variable are usually the stator current components which become

$$i_{ds} = \frac{1}{M}\,(1 + p\,\tau_r)\,\Phi_r \tag{6}$$

$$i_{qs} = \frac{L_r}{M}\,\frac{T}{\Phi_r} \tag{7}$$

Utilising the stator flux components as control variables [5], it is possible to derive two equations similar to (6) and (7). For this purpose it is convenient to solve Eq. (4) for i_s and Eq. 2 for i_r. Substituting the expressions so obtained in Eq. 3 leads to

$$\Phi_{ds} = \frac{L_s}{M}\,(1 + p\,\sigma\,\tau_r)\,\Phi_r \tag{8}$$

$$\Phi_{qs} = \frac{L_r}{M}\,\sigma L_s\,\frac{T}{\Phi_r} \tag{9}$$

where $\sigma = 1 - \dfrac{M^2}{L_s L_r}$ is the leakage coefficient.

In this case the rotor flux control variable is Φ_{ds} while the torque control variable is Φ_{qs}.
It should be noted that this approach has the advantage of requiring the quantities L_s/M and L_r/M which are moderately affected by saturation and the total leakage coefficient σL_s which is slightly dependent on the current, owing to saturation effects.

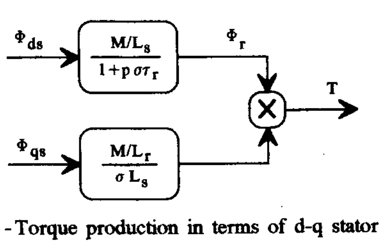

Fig. 1 - Torque production in terms of d-q stator flux component.

Furthermore, a change in flux command is followed whit a time constant $\sigma\tau_r$ which is much lower than the rotor time constant τ_r involved in stator current control. These results are represented in block diagram form in Fig. 1.

TORQUE AND FLUX VECTOR CONTROL STRATEGY

The input commands of the control system are the torque and rotor flux. Considering Eq. 8 written in steady state and Eq. 9, it is possible to determine a relationship between the torque reference T^*, the rotor flux reference Φ_r^* and the stator flux reference Φ_s^*

$$\Phi_s^{*2} = \Phi_{ds}^{*2} + \Phi_{qs}^{*2} = \left(\frac{L_s}{M}\Phi_r^*\right)^2 + (\sigma L_s)^2\left(\frac{L_r}{M}\frac{T^*}{\Phi_r^*}\right)^2 \tag{10}$$

Once the magnitude of the desired stator flux Φ_s^* is determined, the space vector control can be implemented according to the desired torque demand T* and the actual values of torque and stator flux.
A block diagram representing the control system of an induction motor is shown in Fig. 2.
The actual value of stator flux can be evaluated from the stator voltage equation in a stator reference frame

$$\bar{\Phi}_s^s = \int_0^t \left(\bar{v}_s^s - R_s\bar{i}_s^s\right)dt + \bar{\Phi}_{so}^s \tag{11}$$

The torque estimation can be carried out employing Eq. 5 written in terms of stator quantities.

$$T = P\,\bar{i}_s^s \cdot j\bar{\Phi}_s^s \tag{12}$$

The actual values of $\bar{v}_s^s$ and $\bar{i}_s^s$ are calculated by using the DC link voltage E, the inverter switching states S_a, S_b and S_c, and the motor line currents i_a and i_c, by the following equations

$$\bar{v}_s^s = \sqrt{\frac{2}{3}}\,E\left(S_a + S_b e^{j2\pi/3} + S_c e^{j4\pi/3}\right) \tag{13}$$

$$\bar{i}_s^s = \sqrt{\frac{2}{3}}\left(i_a + i_b e^{j2\pi/3} + i_c e^{j4\pi/3}\right) \tag{14}$$

with $i_b = -(i_a + i_c)$.

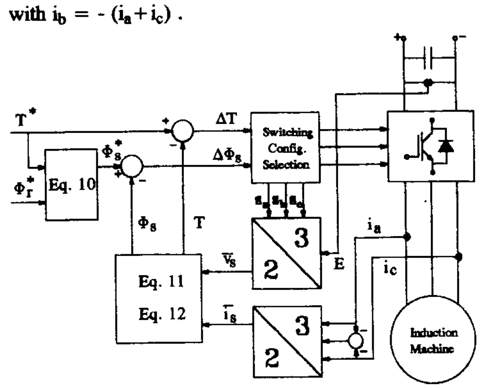

Fig. 2 - Block diagram of the control system.

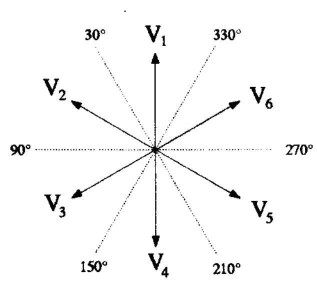

$\vec{v}_s^s$	sector k =	angle	S_a S_b S_c
V_1	1	330° ÷ 30°	1 0 0
V_2	2	30° ÷ 90°	1 1 0
V_3	3	90° ÷ 150°	0 1 0
V_4	4	150° ÷ 210°	0 1 1
V_5	5	210° ÷ 270°	0 0 1
V_6	6	270° ÷ 330°	1 0 1
V_0	-	-	0 0 0
V_7	-	-	1 1 1

Fig. 3 - Inverter output voltage vectors and 60° sectors.

In Fig. 2 the switching configuration selection block determines the state of the inverter switches on the basis of the instantaneous errors in torque ΔT and flux $\Delta\Phi_s$. According to the combination of the switching modes, the voltage vectors are specified for eight kinds of vectors V_k , two of which are zero voltage vectors (V_0 and V_7) and the remaining six are equally spaced voltage vectors having the same magnitude (see Fig. 3). The selection of the proper voltage vector is made in order to maintain the torque and the stator flux within the limits of two hysteresis bands ΔT^* and $\Delta\Phi_s{}^*$ respectively. The inverter switching frequency is closely related to the amplitude of torque and flux hysteresis bands.
It has been shown that the fastest torque response can be obtained by applying the maximum instantaneous slip angular frequency to stator flux [2].

Neglecting the stator IR drop, the trajectory of $\vec{\Phi}_s^s$ moves in the direction of the inverter output voltage vector. Then, the voltage vector which determines the maximum angular acceleration should be selected. According to this statement, to increase the torque value only two voltage vectors can be chosen, which are V_{k+1} or V_{k+2} when $\vec{\Phi}_s^s$ lies in the k-th sector. The selection of one of them is made so that the error of stator flux magnitude satisfies to be within the band limits. In particular, the increase of Φ_s is obtained selecting V_{k+1}, while the decrease of Φ_s is obtained selecting V_{k+2} .
In order to decrease the torque value, it appears evident that voltage vectors V_{k-1} or V_{k-2} should be applied. This choice leads to the fastest decrease torque response but introduces large torque ripple and high commutation frequency. To reduce these drawbacks, zero voltage vector (V_0 or V_7) should be introduced. Utilising zero voltage vectors only, as proposed in [2], a field weakening has been observed, especially at low speed operation, owing to the relevant influence of the stator IR drop. To keep up the stator flux, the voltage vector V_k should be also introduced. In particular, when the flux magnitude is to be increased V_k is selected, when the flux magnitude is to be decreased V_0 or V_7 is selected according to the minimum commutation number of the switches.
The flow-chart of the switching configuration selection algorithm is shown in Fig. 4.
A similar control strategy can be utilised for negative torque reference.

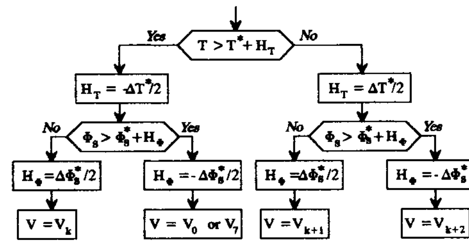

Fig. 4 - Switching configuration selection algorithm for $T^* > 0$ and $\vec{\Phi}_s$ in the k-th sector.

MOTOR PARAMETER SENSITIVITY

The proposed control system basically requires the estimation of stator flux and the evaluation of stator flux reference.
The calculation of the stator flux requires the knowledge of the stator resistance. The effect of an error in R_s is usually quite negligible at high excitation frequency but becomes more serious as the frequency approaches zero. This can be emphasised considering the stator voltage equation written in a stator reference frame and in steady state

$$\vec{v}_s^s = R_s \vec{i}_s^s + j\,\omega_s \vec{\Phi}_s^s \tag{15}$$

where ω_s is the stator angular frequency. Rewriting Eqs. 12 and 15 in terms of error variables results in

$$\Delta T = \frac{i_s^2}{\omega_s} \Delta R_s \tag{16}$$

$$\Delta\vec{\Phi}_s^s = j\frac{\vec{i}_s^s}{\omega_s} \Delta R_s \tag{17}$$

Eqs. 16 and 17 clearly show the influence of ω_s on steady state torque and flux errors. Therefore, the speed range of the drive is limited unless resistance estimation or tuning is incorporated [5].
The evaluation of the stator flux reference requires the knowledge of the total leakage inductance σL_s (Eq. 10).

Unlike R_s , an error in σL_s has the same effect at all excitation frequencies, where it is zero when the torque command is zero and becomes worse under load. It is therefore very important to minimise the error in the value of σL_s . A detailed study exploring the possibility of σL_s tuning will be the subject of future work.

IMPLEMENTATION OF THE CONTROL SCHEME

The direct torque control scheme has been implemented on an interrupt-based program for DSP, the flowchart of which is shown in Fig. 5.

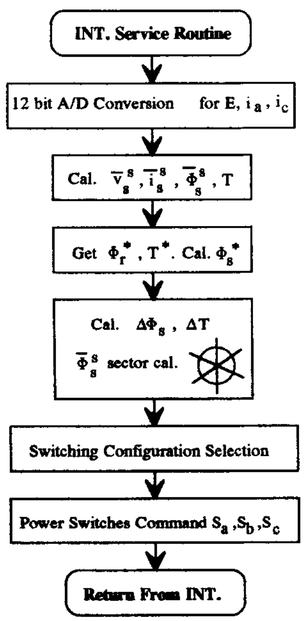

Fig 5 - Flow chart of the interrupt service routine.

Owing to the simplicity of the calculation required, the sampling period is set to 50 μs. The acquisition of the two line currents (i_a, i_c) and of the DC link voltage (E) uses hall-effect sensors associated with analog-to-digital conversion having an accuracy of 12 bit. The calculations are performed on the basis of a 16 bit accuracy.

After the sampling of line motor currents and DC link voltage, the calculation of $\bar{v}_s^s$ and $\bar{i}_s^s$ is performed by Eqs. 13 and 14. Then the actual values of stator flux vector and torque can be evaluated by Eqs. 11 and 12. The reference of stator flux is determined from the commanded values of rotor flux and torque according to Eq. 10.

The switching configuration selection is defined by three input variables: the stator flux error, the torque error and the number of the 60° sector (k) containing the stator flux vector. The output variables are the switching commands S_a , S_b , S_c of the three inverter legs (Fig. 4).

NUMERICAL SIMULATIONS

The good performance of the proposed control scheme has been tested by numerical simulations. To analyse real phenomena such as the sampling period the influence of discretization and of the delay caused by the sampling of signals, the effects of sensors and of analog-to-digital converters, a numerical simulation of the whole system has been carried out. The realistic simulation allows to anticipate an appropriate hardware structure.

The numerical simulations are obtained by integrating the differential equations of the machine model using the 4-th order Runge-Kutta method. The estimations required by the control algorithm are performed at each sampling period of 50 μs. The inverter switch states are updated 30 μs after the acquisitions. The interlock delay and the voltage drop across power switches are neglected.

The test machine is a standard 4 kW , 2-pole, 220V , 50 Hz cage induction motor having the following parameters:

$R_s = 0.402\ \Omega$ $\quad R_r = 0.307\ \Omega$

$L_s = 87.9$ mH $\quad L_r = 89.2$ mH $\quad M = 84.8$ mH

The DC link voltage level is 310 V, the speed value is 100 rad/s and is kept constant during transients.

The performance of the proposed control scheme is tested by evaluating the torque and rotor flux step response.

To emphasise the high overload capability of the drive, a step change in torque command from 50% to 300% of the rated motor torque has been considered. Fig. 6 shows the output torque and stator current magnitude, while Fig. 7 shows the stator and rotor flux loci during the same time interval.

As it is possible to see tne rise time of the torque is about 3 ms and the rotor flux locus is a circle. The stator flux locus shows the increase in flux magnitude required to maintain the rotor flux magnitude fixed to the commanded value.

With reference to a step demand in rotor flux command, Fig. 8 shows the stator and rotor flux magnitude responses. This figure demonstrates the good dynamic performance of the drive obtained without the need of a closed-loop regulation. Fig. 9 shows the torque and the stator current transients due to the change in rotor flux. While the torque maintain the required constant value, the stator current magnitude firstly increases to set the stator flux to the final value, then it decreases as the rotor flux increases.

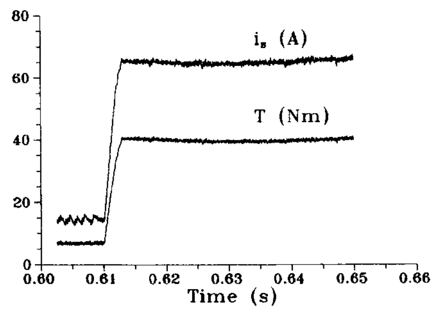

Fig. 6 - Torque and current magnitude during torque step response.

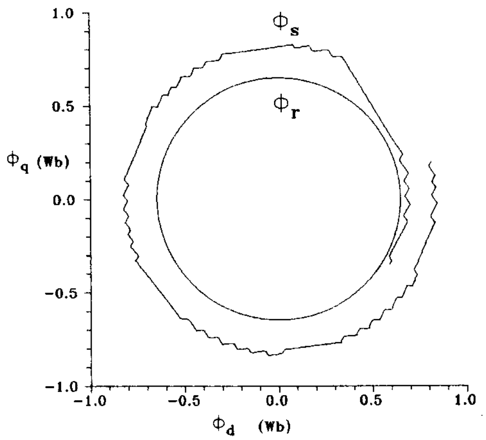

Fig. 7 - Stator and rotor flux loci during torque step response.

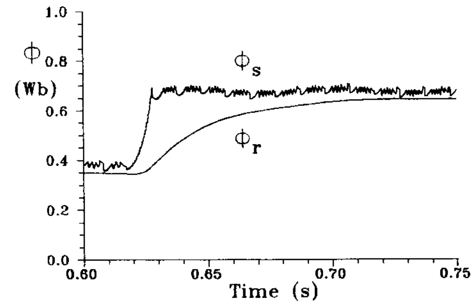

Fig. 8 - Stator and rotor flux magnitude response for a step change in rotor flux command.

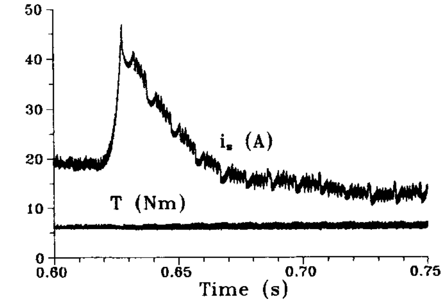

Fig. 9 - Stator current magnitude and torque response for a step change in rotor flux command.

EXPERIMENTAL RESULTS

An experimental drive system was built and tested using the direct control technique, which has been described. The experimental set-up includes a fully digital controlled IGBT inverter and a 4 kW standard induction motor. The main switches are rated at 1000 V, 50 A. For the realisation of the proposed control system, a DSP based processing system has been chosen. It comprehends a 1 MHz, 8-channel 12-bit A/D converter, 2-channel 16-bit D/A converter and a 20 MHz TMS320E15 signal processor. The block diagram of the overall system is shown in Fig. 10. The required computational time allows 20 kHz sampling frequency, leaving enough time for additional computation such as parameter adaptation, filtering routine, protection and diagnostic facility.

The experimental results obtained in steady-state and transient conditions are given in Figs. 11, 12, 13 and 14. These figures have been obtained by converting the digital estimated values to analog form using 16-bit D/A converters. Fig. 11 shows the locus of the stator flux in the steady state at 100 rad/s. In Fig. 12, the locus of the rotor flux is shown for same operating conditions as Fig. 11. Φ_s is controlled to be within the limits of hysteresis band, the irregularities corresponding to commutation processes. The locus of Φ_r is practically a circle owing to the influence of the time constant $\sigma\tau_r$. Fig. 13 shows the torque step response. The torque changes from 20% to 100% of its rated value, at 100 rad/s. It can be seen from Fig. 13 that a quick torque response is obtained. Finally, a torque reference alternating between 30% to 100% of rated value is applied to the system.

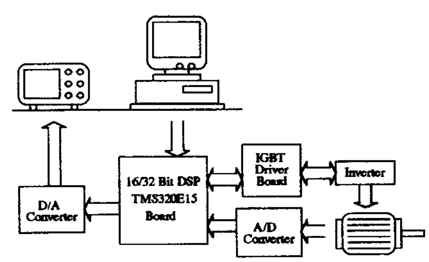

Fig. 10 - Hardware block diagram of the experimental system.

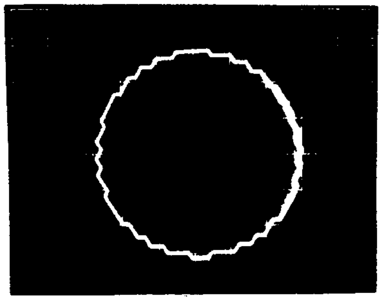

Fig. 11 - Stator flux locus, steady state, ω_m = 100 rad/s.

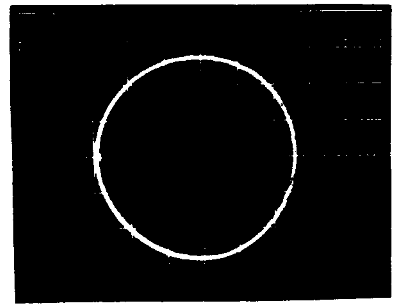

Fig. 12 - Rotor flux locus, steady state, ω_m = 100 rad/s.

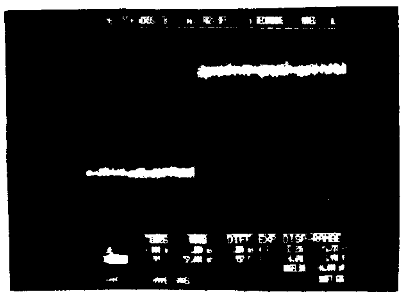

Fig. 13 - Torque step response, 20% to 100% of rated value, ω_m = 100 rad/s.

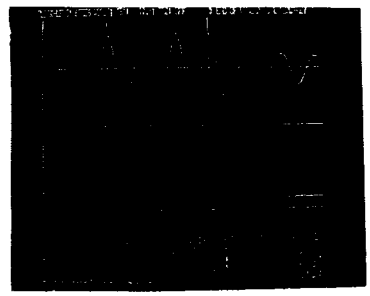

Fig. 14 - Line current and torque for a torque demand 30%→ 100%→ 30%, ω_m = 100 rad/s.

The response is shown in Fig. 14. The top trace represents the instantaneous value of a line stator current, while the bottom trace shows the estimated value of torque.

CONCLUSIONS

This paper was aimed at developing a simplified and efficient digital vector controller for induction machines. The torque control described is based on rotor flux orientation but uses stator flux components as controlled variables. This type of torque control has some advantages. The overload torque capability is increased in comparison with stator flux oriented torque control. The use of stator flux components as controlled variables results in a very simple control scheme which does not require rotor resistance and coordinate transformation based on rotor flux orientation. The scheme presented is very simple to be implemented without the need of speed or position sensors. The total time to read in the data, execute the software and output the switching state to the inverter is about 30μs. With a sampling frequency of 20 kHz it is then available enough time for additional computation such as parameter adaptation. The experimental results clearly demonstrate the feasibility and the good performance of the proposed control scheme.

REFERENCES

[1] H. Baush, R. Blumel, W. Zeng: *Flux-estimation of a PWM-inverter-fed torque-controlled induction machine base on terminal quantities.* ICEM '92, Manchester (UK), September 15-17 1992, Proc. pp. 833-837.

[2] I. Takahashi, T. Noguchi: *A new quick-response and high-efficiency control strategy of an induction motor.* IEEE Trans. on Industry Applications, Vol IA-22, No. 5, September/October 1986, pp 820-827.

[3] I. Takahashi, T. Kanmachi: *Ultra-wide speed control with a quick torque response AC servo by a DSP.* EPE '91, Florence, Italy, September, 3-6 1991, Proc. Vol. III, pp. 572 - 577.

[4] F. Profumo, M. Pastorelli, P. Ferraris, R.W. De Doncker: *Comparison of Universal Field Oriented (UFO) controller in different reference frames.* EPE '91, Florence, Italy, September, 3-6 1991, Proc. Vol. IV, pp. 689- 695.

[5] E. Akin, H. Bulent Ertan, M. Y. Uçtug: *Vector control of induction motor through rotor flux orientation with stator flux components as reference.* ICEM '92, Manchester (UK), September 15-17 1992, Proc. pp. 853-857.